Acta virologica **66**: 324 – 331, 2022 doi: 10.4149/av_2022_403

RT-qPCR based determination of SARS-CoV-2 in health care workers, Cologne, Germany – A pre-delta/pre-omicron proof of principle field study

Gina Spölgen, Jessica Lüsebrink, Verena Schildgen, Oliver Schildgen*

Kliniken der Stadt Köln, Institut für Pathologie, Klinikum der Privaten Universität Witten/Herdecke, Cologne, Germany

Received June 13, 2022; revised July 13, 2022; accepted August 11, 2022

Summary. – The severe acute respiratory syndrome coronavirus 2 (SARS-CoV-2), causing coronavirus disease 2019 (COVID-19), and SARS-CoV-2 variants pose an increased risk to global health. Therefore, monitoring of SARS-CoV-2 variants of concern (VOCs) is of high importance for the implementation of disease control methods, for timely public health decisions, and the development of vaccines against SARS-CoV-2 variants. In this study, which was performed before the delta and omicron variants of concern became dominant, a total of 111 SARS-CoV-2 positive samples from our hospital staff in Cologne, Germany, collected from March 2020 to May 2021 were analysed for VOCs. For determination of VOCs, mutation genotyping analysis (MGA) using mutation-specific simple (MSS) probes based on quantitative reverse transcription-polymerase chain reaction (RT-qPCR) of ten spike protein variants (SPVs) was performed. The MGA focuses on the detection of the spike protein mutation (SPM) of SPVs belonging to VOCs. By successful determination of SPV, the work concludes that 24.66 % of the samples belong to VOC B.1.1.7 and 1.37 % of the samples belong to VOC B.1.351. Based on these results, MGA proves to be a suitable alternative to sequencing technologies as it is a rapid, cost-effective, widely available, and feasible method that allows high sample throughput for the determination of circulating and monitored SARS-CoV-2 VOCs. With focus on the novel variants such as SARS-CoV-2 omicron BA.4 and BA.5 similar approaches could be used for a rapid initial screening, while, however, due to the increasing number of single nucleotide polymorphisms that determine the variants of concern in depth screening becomes more cost efficient by next generation sequencing.

Keywords: COVID-19; SARS-CoV-2; B.1.1.7; B.1.351; spike protein variation; mutation genotyping analysis; RT-qPCR

Introduction

The global corona pandemic caused by SARS-CoV-2 remains a global health challenge that became more complicated by the occurrence of so-called variants of concern (VOCs). On January 5th, 2021, the WHO announced the discovery of two novel variants of SARS-CoV-2. The first variant was detected in the United Kingdom (B.1.1.7) and the second in South Africa (B.1.351) (WHO, 2021b). In mid-March 2021, three VOCs, B.1.1.7; B.1.351, and P.1, were recognised by WHO (WHO, 2021d). About two months later, in May 2021, another VOC (B.1.617.2) was added to the already known variants (WHO, 2021c).

In general, the number of SARS-CoV-2 cases and deaths and the emergence of new variants increased enormously in this short period, either by the pure increasing number of infected individuals or by altered pathogenicity. In any case, it became an internationally accepted strategy to monitor the occurrence and spread of novel variants. In order to address this strategy and fulfil local requirement for strain typing while taking into account economic

*Corresponding author. E-mail: schildgeno@kliniken-koeln.de, oliver.schildgen@uni-wh.de; phone: +49(0)221–890713467.

Abbreviations: MGA = mutation genotyping analysis; MSS = mutation-specific simple; SARS-CoV-2 = severe acute respiratory syndrome coronavirus 2; SPM = spike protein mutation; SPV = spike protein variant; VOCs = variants of concern

considerations that had to avoid high costs of next generation sequencing, this study aimed to validate a rapid, cost-effective, widely available, and feasible PCR-based genotyping analysis that allows high sample throughput and provides an alternative method to sequencing technologies for the determination of the circulating and monitored SARS-CoV-2 VOCs.

Similar approaches have been meanwhile described from several countries in which VOC monitoring was also performed by specific melting curve analyses of RT-q-PCRs, either from patient samples but also from wastewater (Ayadi *et al.*, 2022; Fabiani *et al.*, 2022; Gomes *et al.*, 2022; Norz *et al.*, 2022; Oloye *et al.*, 2022; Sit *et al.*, 2022). Although some of these reports have also considered novel VOCs including omicron and delta, the experience from our setting may be useful.

While in this report, the usage of a set of qPCRs for typing of alpha, beta, and gamma variants is described in the pre-delta and pre-omicron phase of the pandemics, the basic principle of identification of the most recent VOCs by PCRs can be applied for future waves, while in depth typing that detects all relevant and known variants of concern is likely to be more economic by next generation sequencing (Donzelli *et al.*, 2022; Flechsler *et al.*, 2022; Nasereddin *et al.*, 2022; Sun *et al.*, 2022). However, rapid qPCR based VOC detection in hospital staff may also rapidly show if local transmission occurs from within or from outside the hospital working setting and may give insights into infection chain if implemented in the early phase of a new VOC's occurrence.

Materials and Methods

Specimen description. All specimens were throat washings obtained from the staff members testing during routine screenings, and specimens used for the analysis were tested positive for SARS-CoV-2 by RT-qPCR (RealStar SARS-CoV-2 Assay, Altona Diagnostics, Germany) as previously described (Malecki *et al.*, 2020). The patient cohort exclusively consisted of staff members working for the City of Cologne Hospital group and were collected at our three major facilities in Cologne (i.e. three clinics, namely the Hospital in Cologne-Holweide, the Children's Hospital, and the Hospital of the Private University of Witten/Herdecke in Cologne-Merheim) before being transported to our laboratory at the location in Cologne-Merheim.

A total of 111 specimens were included for genotyping analysis. The samples were collected in the period from March 24th, 2020 (week 13, 2020), to May 5th, 2021 (week 18, 2021). The Ct values of the SARS-CoV-2 obtained by the RealStar PCR assays ranged from 12.29 to 39.61 for the spike gene (S-gene) and from 12.40 to 41.05 for the envelope gene (E-gene). The average Ct value of the tested samples for E-gene was 25.00 and for the S-gene 24.37. In 12 specimens with only a single gene tested positive by the RealStar assay, five specimens had no Ct value detected for the E-gene and seven had no Ct value detected for the S-gene.

Mutation genotyping assay. The MGA was performed using a set of commercially available assays (VirSNiP mutations assays, TibMolbiol, Berlin, Germany). The following assays according to figure 1 were used: RT-qPCR for SPV H69/V70 del, K417N, N439K, Y453F, E484K, N501Y, A570D, D614G, P681H, and V1176F. Assays for novel omicron variants as shown in Figure 1 were not available during the study period. All used assays were performed exactly as recommended by the manufacturer's protocols.

Ethics statement. Reporting of this data was covered by governmental general disposition act of the German Ministry of Health (Bundesgesundheitsministerium, 2021).

Data recording/processing software and statistical evaluation tools. Recording and processing of the data generated by RT-qPCR for the determination of SPVs were conducted with the LightCycler ® 480 SW – user defined workflow for COBAS z 480 software (version 1.5.1.62 SP2 – UDF v2.0.0, Roche, Germany). The recording and processing of the data obtained by RT-qPCR for the Ct determination of SARS-CoV-2 were performed by Q-Rex software (version 1.1.0.4) from Qiagen. The data collected in both analyses were entered and organised in Microsoft® Excel® for Microsoft 365 MSO software (version 2112 Build 16.0.14729.20224) from Microsoft.

Genotyping RT-qPCRs. The analysis was carried out by usage of several combined RT-qPCR assays (TIB MolBiol, Germany). In particular, probe-based RT-qPCR for spike protein variants (SPV) relevant for strain identification were H69/V70 del, K417N, N439K, Y453F, E484K, N501Y, A570D, D614G, P681H, and V1176F (Table 1). RNA was extracted from throat washings by using the Promega Maxwell total viral nucleic acid kit (Promega,

Table 1. Description of the SPV used in this study

SPV	Nucleotide variation	Amino acids with codon	
		SPWT	SPM
H69/V70 del	del21765–770	H=His (cat) V=Val (gtc)	deletion of H and V
Y453F	A22920T	Y=Tyr (t**a**t)	F=Phe (t**t**t)
E484K	G23012A	E=Glu (**g**aa)	K=Lys (**a**aa)
N501Y	A23063T	N=Asn (**a**at)	Y=Try (**t**at)
A570D	C23271A	A=Ala (g**c**t)	D=Asp (g**a**t)
D614G	A23403G	D=Asp (g**a**t)	G=Gly (g**g**t)
P681H	C23604A	P=Pro (c**c**t)	H=His (c**a**t)
V1176F	G25088T	V=Val (**g**tt)	F=Phe (**t**tt)

Spike protein variation (SPV) with corresponding nucleotide variation at the nucleotide position and corresponding spike protein wild type (SPWT) amino acid and spike protein mutation (SPM) amino acid with its codon used in this work. The highlighted letter in the codons of SPWT and SPM represents the nucleotide exchange between them.

Spike	Genetic	Variant	Cat.-No.	Alpha	Beta	Gamma	Delta	Lambda	Mu	BA.1	BA.1.1	BA.2	BA.4/5
H66D d69/70	C21758G+del	B.1	53-0801-96	○						○	○		
A67V d69/70	C17762T+del	BA.1	53-0828-96	○						●	●		○
del69/70	del21765-21770	Alpha	53-0781-96	●						○	○		●
C136F	G21969T	C.1.2	53-0821-96										
144del	del21991-21993	Alpha	53-0811-96	●			○		○				
145H	T21995C	AY4.2	53-0823-96	○			●		○				
ins214EPE	22205GAGCCAGAA	BA.1	53-0826-96							●	●		
A222V	C22227T	AY4.2	53-0822-96				●						
del247-253	del22299-22319	Lambda	53-0816-96					●					
D253G	A22320G	B.1.526	53-0800-96										
G339D	G22578A	Omicron	53-0833-96							●	●	●	●
R346K	G22599A	Mu	53-0815-96						●		●		
S371L+S373P	T22673C, C22674T,	BA.1, BA.2	53-0827-96							●		○	○
S371F+S373P+L452R	T22679C, T22917G	BA.1, BA.2, BA.4/.5 Delta	53-0831-96				●			○		●	●
Y449H	T22907C	C.1.2	53-0820-96										
L452R	T22917G	Delta	53-0793-96				●						●
E452Q	T22917A	Lambda	53-0814-96				○	●					○
Y453F	A22920T	Mink	53-0783-96				○						○
K417N	G22813T	Beta	53-0787-96		●	○				●	●	●	●
K417T	A22812C	Gamma	53-0817-96		○	●				○	○	○	○
T478K	C22995A	Delta	53-0813-96				●			○	○	○	○
E484K	G23012A	Beta	53-0789-96		●	●			●	○	○	○	○
E484Q	G23012C	Kappa	53-0809-96		○	○			○	○	○	○	○
E484A	A23013C	BA.1/2	53-0829-96		○	○			○	●	●	●	○
E484A 486V	A23013C, T23018G	BA.4/5	53-0839-96		○	○			○	○	○	○	●
N501Y	A23063T	Alpha, Beta, Gamma	53-0780-96	●	●	●			●	○	○	○	○
N501Y Y505H	A23063T T23075C	Omicron	53-0830-96	○	○	○			○	●	●	●	●
T547K	C23202A	BA.1	53-0832-96							●			
A570D	G23012C	Alpha	53-0791-96	●									
D614G	A23403G		53-0782-96	●	●	●	●	●	●	●	●	●	●
P681H	C23604A	Alpha	53-0786-96	●			○		●	○	○	○	○
P681R	C23604G	Delta	53-0806-96	○			●			○	○	○	○
F888L	T24224C	Eta	53-0798-96										
Q949R	A24409G	B.1	53-0803-96										
I1221T	T25224C	BA.2.2	53-0835-96									●	
V1176F	G25088T	Gamma	53-0784-96			●							

● Hit ○ Secondary Hit ▪ Assays with same target region (overlapping probe)

Fig. 1

Overview of VirSNiP assays for the determin

The scheme is also available online (https://www.tib-molbiol.de/fileadmin/user_upload/Covis-19/VirSNiP/220613_Covid_Tabelle.svg) and was kindly provided for re-usage by TIB Molbiol (Olfert Landt, personal communication, with permission).

Table 2. Variants of concern (VOC) circulating during the sampling period of this study

	WHO label	PANGO lineage	GISAID	Nexstrain	Earliest documented sample	Date of designation
VOC	Alpha	B.1.1.7	GR/ 501Y.V1 (GRY)	20I/ 501Y.V1	United Kingdom (UK), Sep-2020	18-Dec-2020
	Beta	B.1.351	GH/ 501Y.V2	20H/ 501Y.V2	South Africa (ZA), May-2020	18-Dec-2020
	Gamma	P.1	GR/ 501Y.V3	20J/ 501Y.V3	Brazil, Nov-2020	11-Jan-2021

Nomenclature systems used for naming of SARS-CoV-2 VOCs. Presentation of the naming of each variant of concern (VOC) by WHO label, PANGO lineage, GISAID and Nextstrain nomenclature system, the date and location of the earliest documented sample and the date of designation of the corresponding WHO label. Based on WHO (2021a).

Germany). The LightCycler ® 480 SW software (Roche), the LightCycler ® Cobas z480 (LC) (Roche) and PCR reagents containing VirSNiP SARS-CoV-2 spike kits for SPVs (TIB Molbiol) and LightCycler Multiplex RNA virus master mix assay (Roche) were used for genotyping.

Results

Overview of the central results of SPV determination

A total of 111 samples were tested by MGA using MSS probe-based RT-qPCR for SPV H69/V70 del, K417N, N439K, Y453F, E484K, N501Y, A570D, D614G, P681H, and V1176F with melting curve analysis to determine Tm values of these SPVs (Table 1). The determination of this mutation patterns allowed discriminating between the variants of SARS-CoV-2 that were circulating during the sampling period of this study (Table 2), which are characterized by several key mutation patterns (Table 3).

Specimens that displayed the SPMs H69/V70 del, Y501, D570, G614, and H681 were categorised as VOC B.1.1.7 (WHO label: alpha). Samples with SPMs N417, K484, Y501, and G614 were assigned as VOC B.1.351 (WHO label: beta). Finally, samples that showed SPMs T417, K484, Y501, and G614 were classified as VOC P.1 (WHO label: gamma). Gamma specimens were not identified during the entire observation period.

In total 65.77% (73/111) of the specimens included in this study were determined for all ten SPVs tested, whereas 34.23% (38/111) were identified as not typable by RT-qPCR, mainly due to the lack of one or more key mutations relevant for the strain identification (Table 4). In three cases (2.7%) all PCRs were successfully performed, but the resulting mutation patterns did not allow a distinct determination of the variant. Figure 2 shows the distribution of the variants among the specimens in which all genotyping PCRs were successfully conducted. The 24.66% (18/73) samples resulted in the detection of VOC B.1.1.7, whereby the mutation pattern H69/V70 del, Y501, D570, G614, and H681 was detected (Fig. 2). In ad-

Table 3. Key mutation patterns of spike protein variations of VOC Alpha, Beta, and Gamma (Based on (Tegally *et al.*, 2021) and (Galloway *et al.*, 2021)

	B.1.1.7	B.1.351	P.1
	H69/V70 del	L18F	L18F
	Y144 del	D80A	T20N
	N501Y	D215G	P26S
	A570D	L424_244L del	D138Y
	D614G	R246I	R190S
SPV	P681H	K417N	K417T
	T761I	E484K	E484K
	S982A	N501Y	N501Y
	D1118H	D614G	D614G
		A701V	H655Y
			T1027I

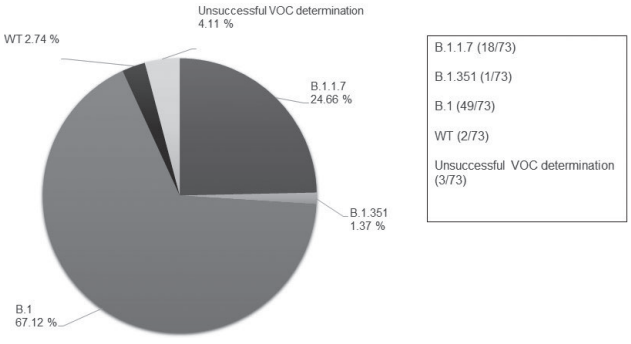

Fig. 2

Distribution of the central results of successful SPV determination

The numbers in brackets indicate the number of samples to which the previous categorisation applies in relation to the successfully tested SPV samples.

dition, the sample chronologically classified as the first VOC B.1.1.7 was collected on February 4th, 2021.

Since that date, all samples that were successful for the strain determination were identified as VOC B.1.1.7.

Furthermore, in 1.37% (1/73) of the successful SPV determination samples, the VOC B.1.351 were determined by detection of the SPMs N417, K484, Y501, and G614. This sample was collected on January 28th, 2021. The remaining 54 samples could not be determined as VOCs. A wild type amino- acid pattern of the type regions known for the Wuhan strain was observed in 2.74% (2/73) of the tested samples, which were accordingly classified as wild type. In addition, these samples were from March 27th and April 1st, 2021. Moreover, while typing for of the mutation G614 a WT pattern for the remaining typed regions was observed in 67.12 % (50/73) of these samples. Since the single presence of the D614G SPV did not indicate a VOC, the Lineage Mutation Tracker was used to search for a matching variant. With this tracker, the samples could be identified as likely belonging to the B.1 lineage (PANGEA_Outbreak_Info, 2022). Moreover, the first sample belonging to B.1 variant dated back to March 24th, 2020.

Furthermore, in 4.11% (3/73) of the samples tested, the spike-protein determination was successful, but SPM was missing to determine a VOC.

Moreover, of the total of 111 samples tested, the RT-qPCR based genotype determination failed for 34.23 % (38/111) of these samples, as amplification errors took place for one or more SPVs, thus the results were classified as invalid according to the manufacturer's protocol. Furthermore, the Ct values of the E-gene and S-gene of the pre-characterised samples as determined by the RealStar RT-qPCR assay (Altona, Germany) were consulted for further analysis. The average of the S-gene Ct values was 30.16 and that of the E-gene Ct values was 29.13. The lowest Ct value for the S-gene was 18.88 (sample 23) and the highest was 41.05 (sample 21). For the E-gene, the lowest Ct value was 18.36 (sample 53) and the highest was 39.61 (sample 23).

Table 4. Results of RT-qPCR based genotyping of SARS-CoV-2 variant

		Number of samples	Percentage of samples (%)	
Successful SPV determination	B.1.1.7	18	16.22	65.77
	B.1.351	1	0.90	
	B.1	49	44.14	
	WT	2	1.80	
	Unsuccessful VOC determination	3	2.70	
Unsuccessful SPV determination (amplification error)		38	34.23	
Total amount of samples		111	100.00	

B.1.1.7, B.1.351, B.1 and wild type (WT) represent the SARS-CoV-2 variants classified by the successful spike protein variant determination. Unsuccessful VOC determination means an insufficient number of spike protein mutations detected to determine an exact variant.

Discussion

Monitoring of variants of concern (VOCs) including their spike protein variations (SPVs) is of high importance for the implementation of disease control methods, timely public health decisions and vaccine development against new variants of SARS-CoV-2 (WHO, 2021c; WHO, 2021d). Tracking SARS-CoV-2 VOCs with sequencing technologies has several limitations, including that it is time-consuming and expensive, needs technical expertise, and is not widely available and feasible (Grubaugh *et al.*, 2021; Wang *et al.*, 2021). Therefore, molecular diagnostic PCR based tests represent an alternative to sequencing techniques to obtain more information about circulating VOCs, as they are cost-efficient, rapid, more readily available, and feasible and allow a high sample throughput. Some studies report on molecular diagnostic tests that indicate the presence of SPM of SPVs. In addition, there are some studies that can also conclude on VOCs independently of confirmation by sequencing. In early 2021, Bal *et al.* (Bal *et al.*, 2021) and Borges *et al.* (Borges *et al.*, 2021) described a method to suspect the H69/V70 deletion by the presence of a spike protein target failure (SPTF) or a spike gene target late detection (SGLT). Furthermore, Wang *et al.* published a study on a one-step multiplex allele-specific qualitative RT-qPCR assay to assume the presence of B.1.1.7 and B.1.351 in their tested samples. The studies by Durner *et al.* (2021), Matic *et al.* (2021) and Camp *et al.* (2021) refer to the same VirSNiP-SARS-CoV-2 spike kit from TIB Molbiol as used in the underlying work. Durner *et al.* (2021) used SPV N501Y, whereas Matic *et al.* (2021) used five SPVs (N501Y, H69/V70 del, K417N, E484K and V1176F) to detect VOC. In the study by Camp *et al.* (2021) 9 laboratories performed an external quality assessment using the four SPVs N501Y, H69/V70 del, K417N and E484K.

In this work, we retrospectively analysed specimens collected during the first three waves of VOC, namely alpha, beta, and gamma variant.

Based on the successful SPV determination, VOC B.1.1.7 could be identified in 24.66 % of the samples while VOC B.1.351 was detected in 1.37%. Furthermore, 2.74% of the 73 samples were identified as full Wuhan wild type while a total of 67.12% could be associated with lineage

B.1, as only the SPM G614 of SPV D614G was detected. In addition, the sample that was chronologically detected for the first time as VOC B.1.1.7 was collected on February 4th, 2021. The samples following the aforementioned date were identified as VOC B.1.1.7. This indicates that from February 4th, 2021, until the end of the analysis, VOC B.1.1.7 was predominant over other variants, at least in our setting. The B.1 lineage was also predominant over the wild type until the first detection of B.1.1.7 and B.1.351, as WT was not detected after the first detection of B.1. Thus, this study was able to confirm Lauring and Hodcraft's statement (Lauring and Hodcroft, 2021) that dominant variants of SARS-COV-2 such as B.1.1.7 could replace existing SARS-CoV-2 populations. Nevertheless, for a total of 34.23% of the samples, amplification failed for some SPV, so the results were classified as invalid. In any case, however, we observed that there was a time gap between the first communication of a newly emerging VOC, the governmental advice to test for this particular variant, and the laboratory assays being available. As a consequence, the novel variant has twice taken over epidemiological dominant role before broad diagnostics were established, and the relevance of qPCR-based typing rapidly vanished.

However, our study has some limitations. First, the number of samples tested was rather low compared to other studies and included 111 specimens, however, all collected form health care staff members. Moreover, due to the lack of staff member capacities and difficulties regarding reimbursement, we were not able to confirm the detected SNPs by next generation sequencing, which we assumed to be a minor weakness as we successfully passed an external quality assessment scheme for SARS-CoV-2 typing (INSTAND e.V., Düsseldorf, Germany; data not shown).

In addition, the retrospective analyses may have been accompanied by a decrease in the RNA quality, although the samples were sufficiently stored at -80° until RNA extraction and subsequent genotyping was performed. However, earlier studies faced similar limitations.

In addition, Matic *et al.* (Matic *et al.*, 2021) implemented TIB Molbiol's VirSNiP-SARS-CoV-2 spike kit for SPV N501Y, H69/V70 del, K417N, E484K and V1176F using samples from Vancouver, British Columbia and Canada. They used two test approaches, whereby SPV N501Y was used for the first test approach to distinguish between wild type and VOCs (B.1.1.7, B.1.351 and P.1) because SPV N501Y is present in all VOCs. Only if this test was positive, these samples were tested with the other SPVs (H69/V70 del, K417N, E484K, V1176F) to distinguish between the VOCs. A total of 2,430 SARS-CoV-2 positive samples were tested.

Of these samples, 38 samples (1.6 %) failed in amplification for SPV N501Y, which Matic *et al.* and (Matic *et al.*, 2021) attributed to late Ct values and low viral load. In total, 57 samples were detected with VOC B.1.1.7, 7 samples with VOC B.1.351, and 13 samples with VOC P.1. Similar to Wang *et al.* (2021), the authors described this testing approach as rapid, with results available within 24 h, as well as cost-effective. They also pointed out that even if the SPV N501Y was present in all known VOCs at the time, other variants that also contained this SPV could remain undetected by this testing approach. Compared to the other studies, this test approach, and the use of the aforementioned test kits from TIB Molbiol allowed the VOCs to be determined directly. Therefore, identification by sequencing would not be necessary. Consequently, this test was sufficient to detect the variants of concern present at that time (Galloway *et al.*, 2021).

The last study by Camp *et al.* (2021) focused on an external quality assessment of 25 laboratories, including 15 laboratories that used the TIB-Molbiol kit. Of the 15 laboratories, a maximum of 11 SPV (H69/V70 del, K417N, N439K, Y453F, E484K, N501Y, A570D, D614G, P681H, F888L, V1176F) were tested. For this study, five samples were pre-tested for SARS-CoV-2 variants using whole genome sequencing (WGS), resulting in the identification of VOCs B.1.1.7, B.1.351, and additional variants, B.1.177, B.1.1.7 + G75V and B.1.258. Of the 15 participating laboratories, all tested SPV were N501Y, 11 tested SPV were H69/V70 del, 11 tested were SPV K417N, and 9 tested SPV were E484K. Samples B.1.1.7 and B.1.351 were identified correctly by all laboratories. Furthermore, for the other samples, false, unclear, and unreported results were obtained for some SPVs. The authors' evaluation showed that one sample (B.1.1.7 + G75V) yielded false test results due to a substitution near SPV H69/V70 del, which caused a change in the melting peaks.

For sample B.1.258, they suspected a test failure, caused by an insufficient amount of the template. Moreover, the authors suggested that the reported unclear results of some laboratories occurred because of the usage of less than four SPVs in screening. Thus, only little information would be available for a successful interpretation. They concluded that, among other tests, the VirSNiP SARS-CoV-2 spike kit was suitable for the classification of VOCs, as VOC B.1.1.7 and VOC B.1.351 were successfully determined by all 15 laboratories. Camp *et al.* pointed out that careful interpretation and quality assurance was highly important for identifying variants. In comparison to the previously reported studies, Camp *et al.* concluded, that a certain number of SPV should be investigated to provide a reliable result for variants. In addition, it was confirmed that, as in other test approaches, other variants could also be determined besides VOCs. In conclusion, in the study by Camp *et al.* (2021) and in Matic *et al.* (2021), the VOCs could also be reliably determined, so that identification

or confirmation by sequencing would theoretically not be necessary (Camp *et al.*, 2021).

In summary, the MGA based on MSS probe RT-qPCR by VirSNiP SARS-CoV-2 spike kit (TIB Molbiol) was suitable for the determination of already known VOCs such as B.1.1.7 and B.1.351 as well as lower priority variants e.g., samples belonging to lineage B.1. However, in order to timely monitor and react on novel variants of concern, more rapid and embracing WGS is required combined with more rapid communication, as e.g. performed in other countries such as UK. With the rapidly upcoming variants of concern, most recently the variants BA.4 and BA.5, one may ask what the most cost-effective strategy will be. Most likely, qPCR-based typing could be used to detect one or two characteristic leader mutations, while next generation sequencing will be the method of choice for in depth determination of variant screenings (Donzelli *et al.*, 2022; Flechsler *et al.*, 2022; Nasereddin *et al.*, 2022; Sun *et al.*, 2022). Additionally, it could be asked if broad routine typing is relevant and superior to random and sporadic monitoring at all unless the clinical severity of the VOCs does not increase.

Acknowledgments. The authors declare that (I) the work did not receive funding, (II) all authors have read and approved the final manuscript and contributed actively to the study, and (III) that none of the authors has any conflict of interest related to this study.

References

Ayadi W, Taktak A, Gargouri S, Smaoui F, Chtourou A, Skouri-Gargouri H, Derbel R, Sassi AH, Gargouri A, Hammami A, Karray-Hakim H, Mokdad-Gargouri R, Fki-Berrajah L (2022): Development of a simple genotyping method based on indel mutations to rapidly screen SARS-CoV-2 circulating variants: Delta, Omicron BA.1 and BA.2. J. Virol. Methods 307, 114570. https://doi.org/10.1016/j.jviromet.2022.114570

Bal A, Destras G, Gaymard A, Stefic K, Marlet J, Eymieux S, Regue H, Semanas Q, d'Aubarede C, Billaud G, Laurent F, Gonzalez C, Mekki Y, Valette M, Bouscambert M, Gaudy-Graffin C, Lina B, Morfin F, Josset L, Group CO-DHS (2021): Two-step strategy for the identification of SARS-CoV-2 variant of concern 202012/01 and other variants with spike deletion H69-V70, France, August to December 2020. Euro Surveill. 26. https://doi.org/10.2807/1560-7917.ES.2021.26.3.2100008

Borges V, Sousa C, Menezes L, Goncalves AM, Picao M, Almeida JP, Vieita M, Santos R, Silva AR, Costa M, Carneiro L, Casaca P, Pinto-Leite P, Peralta-Santos A, Isidro J, Duarte S, Vieira L, Guiomar R, Silva S, Nunes B, Gomes JP (2021): Tracking SARS-CoV-2 lineage B.1.1.7 dissemination: insights from nationwide spike gene target failure (SGTF) and spike gene late detection (SGTL) data, Portugal, week 49 2020 to week 3 2021. Euro Surveill. 26. https://doi.org/10.2807/1560-7917.ES.2021.26.10.2100130

Bundesgesundheitsministerium (2021): Verordnung zur molekulargenetischen surveillance des Coronavirus SARS-CoV-2 (Coronavirus-Surveillanceverordnung-CorSurV): BAnz AT 19.01.2021 V2. Bundesanzeiger.

Camp JV, Buchta C, Jovanovic J, Puchhammer-Stockl E, Benka B, Griesmacher A, Aberle SW, Goerzer I (2021): RT-PCR based SARS-CoV-2 variant screening assays require careful quality control. J. Clin. Virol. 141, 104905. https://doi.org/10.1016/j.jcv.2021.104905

Donzelli S, Ciuffreda L, Pontone M, Betti M, Massacci A, Mottini C, De Nicola F, Orlandi G, Goeman F, Giuliani E, Sperandio E, Piaggio G, Team IC, Morrone A, Ciliberto G, Fanciulli M, Blandino G, Pimpinelli F, Pallocca M (2022): Optimizing the Illumina COVIDSeq laboratorial and bioinformatics pipeline on thousands of samples for SARS-CoV-2 variants of concern tracking. Comput. Struct. Biotechnol. J. 20, 2558–2563. https://doi.org/10.1016/j.csbj.2022.05.033

Durner J, Burggraf S, Czibere L, Tehrani A, Watts DC, Becker M (2021): Fast and cost-effective screening for SARS-CoV-2 variants in a routine diagnostic setting. Dent Mater 37, e95-e97. https://doi.org/10.1016/j.dental.2021.01.015

Fabiani M, Margiotti K, Sabatino M, Viola A, Mesoraca A, Giorlandin C (2022): A rapid and consistent method to identify four SARS-CoV-2 variants during the first half of 2021 by RT-PCR. Vaccines (Basel) 10. https://doi.org/10.3390/vaccines10030483

Flechsler J, Eberle U, Dangel A, Hepner S, Wimmer C, Lutmayr J, Konrad R, Berger C, Weise L, Sprenger A, Zeitler J, Paravinja N, Angermeier H, Githure G, Schmidt S, Treis B, Okeyo M, Liebl B, Ackermann N, Sing A, Bavarian S-C-PHLT (2022): Molecular SARS-CoV-2 surveillance in Bavaria shows no Omicron transmission before the end of November 2021. Infection 50, 761–766. https://doi.org/10.1007/s15010-022-01767-1

Galloway SE, Paul P, MacCannell DR, Johansson MA, Brooks JT, MacNeil A, Slayton RB, Tong S, Silk BJ, Armstrong GL, Biggerstaff M, Dugan VG (2021): Emergence of SARS-CoV-2 B.1.1.7 Lineage – United States, December 29, 2020-January 12, 2021. MMWR Morb. Mortal. Wkly Rep. 70, 95–99. https://doi.org/10.15585/mmwr.mm7003e2

Gomes L, Jeewandara C, Jayadas TP, Dissanayake O, Harvie M, Guruge D, Withanage V, Mahesh PKB, Rajapakse W, Ramachandran R, Dharmarajan V, Pathiraja I, Sanjeewani A, Bandara P, Nanayakkara G, Francis VR, Kithsiri A, Edirisinghe DA, De Silva K, Wijayamuni R, Ogg GS, Waggoner J, Malavige GN (2022): Surveillance of SARS-CoV-2 variants of concern by identification of single nucleotide polymorphisms in the spike protein by a multiplex real-time PCR. J. Virol. Methods 300, 114374. https://doi.org/10.1016/j.jviromet.2021.114374

Grubaugh ND, Hodcroft EB, Fauver JR, Phelan AL, Cevik M (2021): Public health actions to control new

SARS-CoV-2 variants. Cell 184, 1127–1132. https://doi.org/10.1016/j.cell.2021.01.044

Lauring AS, Hodcroft EB (2021): Genetic variants of SARS-CoV-2-what do they mean? JAMA 325, 529–531. https://doi.org/10.1001/jama.2020.27124

Malecki M, Lusebrink J, Teves S, Wendel AF (2020): Pharynx gargle samples are suitable for SARS-CoV-2 diagnostic use and save personal protective equipment and swabs. Infect. Control. Hosp. Epidemiol. 1–2. https://doi.org/10.1017/ice.2020.229

Matic N, Lowe CF, Ritchie G, Stefanovic A, Lawson T, Jang W, Young M, Dong W, Brumme ZL, Brumme CJ, Leung V, Romney MG (2021): Rapid detection of SARS-CoV-2 variants of concern, including B.1.1.28/P.1, British Columbia, Canada. Emerg. Infect. Dis. 27, 1673–1676. https://doi.org/10.3201/eid2706.210532

Nasereddin A, Golan Berman H, Wolf DG, Oiknine-Djian E, Adar S (2022): Identification of SARS-CoV-2 variants of concern using amplicon next-generation sequencing. Microbiol. Spectr. e0073622. https://doi.org/10.1128/spectrum.00736-22

Norz D, Grunwald M, Tang HT, Weinschenk C, Gunther T, Robitaille A, Giersch K, Fischer N, Grundhoff A, Aepfelbacher M, Pfefferle S, Lutgehetmann M (2022): Clinical evaluation of a fully-automated high-throughput multiplex screening-assay to detect and differentiate the SARS-CoV-2 B.1.1.529 (Omicron) and B.1.617.2 (Delta) lineage variants. Viruses 14, 10. https://doi.org/10.3390/v14030608

Oloye FF, Xie Y, Asadi M, Cantin J, Challis JK, Brinkmann M, McPhedran KN, Kristian K, Keller M, Sadowski M, Jones PD, Landgraff C, Mangat C, Fuzzen M, Servos MR, Giesy JP (2022): Rapid transition between SARS-CoV-2 variants of concern Delta and Omicron detected by monitoring municipal wastewater from three Canadian cities. Sci. Total Environ. 841, 156741. https://doi.org/10.1016/j.scitotenv.2022.156741

PANGEA_Outbreak_Info (2022): Lineage Mutation Tracker: B1 Lineage Report; https://outbreak.info/situation-reports?pango=B.1

Sit BHM, Po KHL, Cheung YY, Tsang AKL, Leung PKL, Zheng J, Lam AYT, Lam ETK, Ng KHL, Chan RCW (2022): Detection of SARS-CoV-2 VOC-Omicron using commercial sample-to-answer real-time RT-PCR platforms and melting curve-based SNP assays. J. Clin. Virol. Plus 2, 100091. https://doi.org/10.1016/j.jcvp.2022.100091

Sun Y, Zhang Y, Liu Z, Li X, Liu J, Tian X, Gao Q, Niu P, Zhai H, Sun Z, Tian Y, Wang J (2022): Analysis of the transmission of SARS-CoV-2 Delta VOC in Yantai, China, August 2021. Front. Med. (Lausanne) 9, 842719. https://doi.org/10.3389/fmed.2022.842719

Tegally H, Wilkinson E, Giovanetti M, Iranzadeh A, Fonseca V, Giandhari J, Doolabh D, Pillay S, San EJ, Msomi N, Mlisana K, von Gottberg A, Walaza S, Allam M, Ismail A, Mohale T, Glass AJ, Engelbrecht S, Van Zyl G, Preiser W, Petruccione F, Sigal A, Hardie D, Marais G, Hsiao NY, Korsman S, Davies MA, Tyers L, Mudau I, York D, Maslo C, Goedhals D, Abrahams S, Laguda-Akingba O, Alisoltani-Dehkordi A, Godzik A, Wibmer CK, Sewell BT, Lourenco J, Alcantara LCJ, Kosakovsky Pond SL, Weaver S, Martin D, Lessells RJ, Bhiman JN, Williamson C, de Oliveira T (2021): Detection of a SARS-CoV-2 variant of concern in South Africa. Nature 592, 438–443. https://doi.org/10.1038/s41586-021-03402-9

Wang H, Miller JA, Verghese M, Sibai M, Solis D, Mfuh KO, Jiang B, Iwai N, Mar M, Huang C, Yamamoto F, Sahoo MK, Zehnder J, Pinsky BA (2021): Multiplex SARS-CoV-2 genotyping reverse transcriptase PCR for population-level variant screening and epidemiologic surveillance. J. Clin. Microbiol. 59, e0085921. https://doi.org/10.1128/JCM.00859-21

WHO (2021a): An update on SARS-CoV-2 virus mutations & variants.

WHO (2021b): Weekly Edpidemiological Update – 5 January 2021, Vol. 2022.

WHO (2021c): Weekly Epidemiological Update on COVID-19 – 1 June 2021.

WHO (2021d): Weekly Epidemiological Update on COVID-19 – 16 March 2021.

Acta virologica **66**: 332 – 338, 2022 doi: 10.4149/av_2022_404

The emerging Omicron variant spike mutation: the relative receptor-binding domain affinity and molecular dynamics

Mahmoud Kandeel[1,2]

[1]Department of Biomedical Sciences, College of Veterinary Medicine, King Faisal University, Al-Hofuf, 31982 Al-Ahsa, Saudi Arabia; [2]Department of Pharmacology, Faculty of Veterinary Medicine, Kafrelshikh University, Kafrelshikh 33516, Egypt

Received January 17, 2022; revised August 8, 2022; accepted August 22, 2022

Summary. – This study aims to fill a knowledge gap in our understanding of Omicron variant receptor-binding domain (RBD) interactions with host cell receptor, angiotensin-converting enzyme 2 (ACE2). Protein-protein docking, scoring, and filtration were all performed using the HDOCK server. A coarse-grained prediction of the changes in binding free energy caused by point mutations in Omicron RBD was requested from the Binding Affinity Changes upon Mutation (BeAtMuSiC) tools. GROMACS was utilized to perform molecular dynamics simulations (MD). Within the 15 mutations in Omicron RBD, several mutations have been linked to increased receptor affinity, immunological evasion, and inadequate antibody response. Wild-type (wt) SARS-CoV-2 and its Omicron variant have 92.27% identity. Nonetheless, Omicron RBD mutations resulted in a slight increase in the route mean square deviations (RMSD) of the Omicron structural model during protein-protein docking, as evidenced by RMSDs of 0.47 and 0.85 Å for the wt SARS-CoV-2 and Omicron RBD-ACE2 complexes, respectively. About five-point mutations had essentially an influence on binding free energy, namely G6D, S38L, N107K, E151A, and N158Y. The rest of the mutations were expected to reduce the binding affinity of Omicron RBD and ACE2. The MD simulation supports the hypothesis that Omicron RBD is more stably bound to ACE2 than wt SARS-CoV-2 RBD. Lower RMSD and greater radius of gyration (Rg) imply appropriate Omicron structure 3D folding and stability. However, the increased solvent accessible surface area (SASA) with a greater Omicron shape may have a different interaction with receptor binding and regulate virus entrance. Omicron RBD's mutations help it maintain its structural stability, compactness, ACE2 binding, and immune evasion.

Keywords: Omicron variant; SARS-CoV-2; COVID-19; phylogenetics

Introduction

There have been more than 577 million confirmed cases and more than 6.4 million deaths in the global coronavirus disease 2019 (COVID-19) pandemic caused by SARS-CoV-2 (WHO COVID-19 pandemic, https://covid19.who.int/, accessed on 2022/8/3). Despite extensive vaccination, the COVID-19 pandemic continues, as SARS-CoV-2 evolves into many forms. Since the November 24th, 2021 discovery of the novel SARS-CoV-2 variation of concern (VOC) Omicron in an immunocompromised patient in South Africa, the variant has quickly surpassed Delta as the most common lineage in the country and spread to over 40 countries (Wang and Cheng, 2022).

Omicron possesses a slew of previously identified mutations in other VOCs, including at least 32 mutations in the spike protein alone (compared to 16 mutations

E-mail: mkandeel@kfu.edu.sa; phone: +966568918734.

Abbreviations: COVID-19 = coronavirus disease 2019; RBD = receptor-binding domain; ACE2 = angiotensin-converting enzyme 2; NSP = nonstructural proteins; MD = molecular dynamic; RMSD = route mean square deviations; Rg = radius of gyration; SASA = solvent accessible surface area

in the already highly infectious Delta form), as well as mutations in other viral replication proteins including nonstructural proteins (NSP), NSP12 and NSP14 (Gao *et al*., 2022). It is possible that SARS-CoV-2 could generate crucial mutations to boost transmission and annul earlier vaccination under the influence of immunological selection (Wang and Cheng, 2022).

Various issues have been raised as a result of the Omicron variant's emergent character, including the source of emergence, the effect of Omicron mutations on vaccination response, the role of mutations on the regulation of host immunity, clinical data, and Omicron spreading potency and lethality. This research aims to 1) determine the impact of Omicron spike mutations on variations in binding free energy between Omicron and the wt SARS-CoV-2 RBD and the host cell receptor ACE2. In this regard, all mutations are studied, including those at the RBD-ACE2 interface and those that do not share the direct virus spike-cell receptor interface. 2) Omicron RBD protein-protein docking with the host ACE2 receptor, and changes in binding confirmation. 3) Wt SARS-CoV-2 and its Omicron variant MD simulation. The analysis criteria include binding stability, changes in protein surface area, protein compactness, and integrity of the 3D structure.

Materials and Methods

Retrieval and handling of Omicron data. The genomes of Omicron variants were retrieved from GISAID website (https://www.gisaid.org/) (Shu and McCauley, 2017). The spike sequence, conversion of DNA to protein, and allocation of RBD sequences were handled by in-house Geneious prime software (Kearse *et al*., 2012).

Structure preparation. In this study, Omicron RBD was built utilizing the previously disclosed structure of wt SARS-CoV-2 RBD in conjunction with the human cell receptor ACE2. The RBD-ACE2 of wt SARS-CoV-2 was obtained from the Protein Data Bank (PDB ID 6m0j). In preparation for docking, water was removed, free forms of RBD and ACE2 were generated and energy was minimized. The Omicron RBD structure was built using the wt SARS-CoV-2 RBD using the SWISS-MODEL server (Waterhouse *et al*., 2018). The resulting RBD was used for template-based homology modeling on the server. The modeling procedure and confirmation of model quality were done as previously described (Kandeel *et al*., 2020, 2021a).

Protein-protein docking. The structure of the Omicron RBD and human ACE2 complex was built using HDOCK server, a hybrid protein-protein docking method (Yan *et al*., 2020). HDOCK uses a fast Fourier transform (FFT)-based search approach to sample all possible binding modes between the interacting partners (He *et al*., 2020). To process the structure by HDOCK program, the wt SARS-CoV-2 RBD and the host receptor ACE2 were used as a starting position. An iterative knowledge-based scoring approach called ITScorePP was used to evaluate all of the binding possibilities that were tested in the sample. The binding modes were sorted according to their binding energy levels at the end of the process, and all viable binding modes were downloaded for further investigation. In the docking computations for the RBD-ACE2, all of the default settings were utilized. In a summary, the grid spacing for 3D translational search was set to 1.2, the angle interval for rotational sampling was set to 15, and the PDB binding interface information for individual structures was automatically utilized during template-based modeling of individual structures.

SARS-CoV-2 spike-receptor interface mutational analysis. Requests for the effect of mutations on spike-RBD binding affinity were submitted to the BeAtMuSiC server (Dehouck *et al*., 2013). The method is based on a coarse-grained prediction of the binding free energy changes that result from point mutations. Mutation-induced changes to the stability of the complex can be predicted by using statistical probabilities that are derived from known protein structures. The input structures were the wt SARS-CoV-2 RBD-ACE2 (6m0j) or wt SARS-CoV-2 RBD spike-ACE2 (7df4) complexes and the Omicron RBD-ACE2 generated structure model.

Molecular dynamic (MD) simulations. To execute molecular dynamics simulations on the protein, GROMACS v. 2021 was used. The simulations made use of the nucleic AMBER94 forcefield and the AMBER99SB-ILDN protein. The protein system composed of 3036 atoms was immersed in a 1.2 nm cubic box containing 3-point model (TIP3P) water, and the complex was ionized using NaCl molecules and neutral pH conditions. Each simulated system was subjected to energy minimization using the steepest descent approach in a maximum of 2000 steps, followed by two stages of equilibration simulations with position restraints. At 310 K, the constant-temperature and constant-volume (NVT) ensemble was used for 100 ps, followed by the constant-temperature and constant-pressure ensemble (NPT). The MD simulation was run for 100 ns at 310 K with no position constraints. Periodic boundary conditions were applied to all directions. Bond limitations were modeled using the LINCS algorithm, with a time step of 2 fs. The PME technique was used to describe short-range nonbonded interactions with a twin-range cutoff of 0.8 nm and long-range electrostatic interactions with a Fourier grid spacing of 0.12 nm. To evaluate simulation results, various GROMACS utilities were utilized. Secondary structure was determined using the do_dssp tool, hydrogen bonds using the hbond tool, surface accessible area using the sasa tool, and gyration using the gyrate tool. The diagrams were created using Grace, and the frames were visualized using Pymol.

Results and Discussion

The location of Omicron variant RBD mutations

In Omicron RBD, there were 15 mutations. Seven mutations were facing the solvent (G6D, S38L, S40P, S42F,

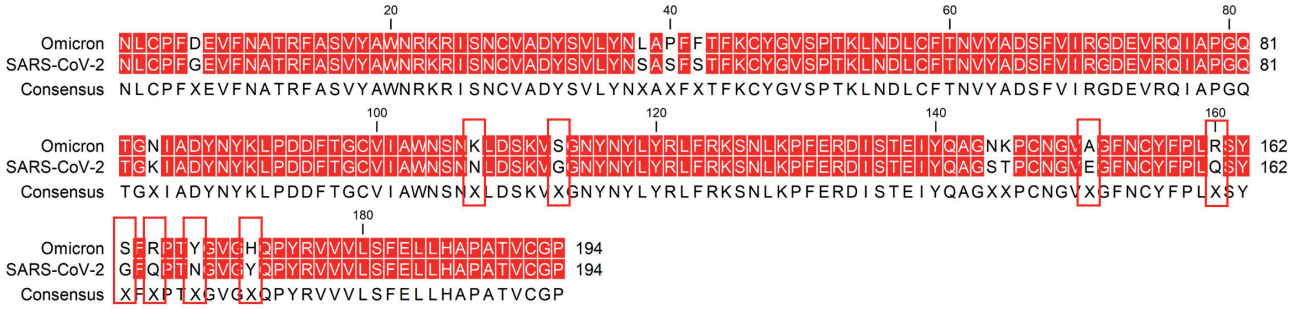

Fig. 1

Pairwise sequence alignment of RBD from wt SARS-CoV-2 and its Omicron variant
The conserved residues are highlighted in red. The mutations at RBD-ACE2 interface are enclosed in boxes.

N107K, S144N, and T145K) and eight mutations were at the RBD-ACE2 interface (K84N, G113S, E151A, G163S, N158Y Q160R, Q165R, and Y172H) (Fig. 1). The significant number of mutations found at the RBD necessitated additional research using mutational analysis of the wt SARS-CoV-2 RBD to determine its impact on binding free energy.

The significance of Omicron mutations

For attachment, fusion and internalization, the SARS-CoV-2 spike glycoprotein interacts with the human ACE2 receptor. As a result, most prophylactic drugs and vaccinations are designed to prevent attachment or entry steps by preventing or neutralizing spike and ACE2 interactions. Therefore, mutations in this part of the virus could be associated with changes in virus infectivity and interfere with the response to immunization. In the Omicron variant, several mutants as K84N, S144N, T145K, E151A, and N158Y were found to improve affinity with receptors or immune escape (Ho *et al.*, 2021; Li *et al.*, 2020; Starr *et al.*, 2020). A shift to basic residues was detected among the eight alterations at the Omicron

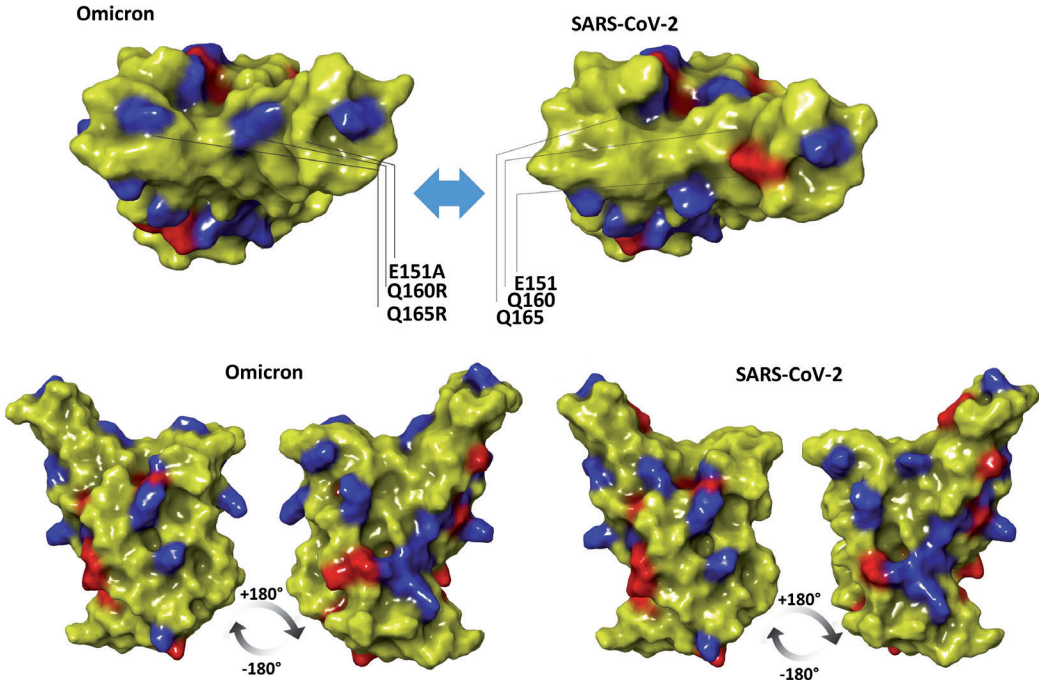

Fig. 2

Surface representation of wt SARS-CoV-2 and Omicron RBD
(a) The interface colored by charge in wt SARS-CoV-2 and Omicron RBD. Positive charge is represented by blue, whereas the negative charge is represented by red. **(b)** The solvent-facing surfaces of wt SARS-CoV-2 and Omicron RBD.

receptor-binding motif. Three acidic residues were found in close proximity to the receptor at the receptor-binding motif, Y172H, Q160R, and Q165R (Fig. 2). At the interface of RBD-ACE2, three important mutations were found E151A, Q160R, and Q165R. More importantly, the formal mutation E151A has been associated with resistance and poor immunological response, while the latter two mutations Q160R and Q165R have been associated with stronger binding with the receptor, inferring higher infectivity (Greaney *et al*., 2021). The susceptibility to pseudotyped Omicron, as well as other variants like Alpha, Beta, Gamma, and Delta, was tested in serum samples from COVID-19 convalescent patients infected with the original SARS-CoV-2 strain. In comparison to 1.2–4.5 folds in other variations, the mean neutralization ED50 of these sera against Omicron was lowered by 8.4 times (Zhang *et al*., 2022). This shows that the Omicron version was able to evade the consolidated immunological response to SARS-CoV-2.

N158Y, E151K, S144N, and most importantly, Q156R were the mutations fixed for increased affinity binding (Zahradnik *et al*., 2021). A large number of mutational changes in Omicron result in a significant decrease in the neutralizing capacity of immunological serum and the failure of immune protection (Dejnirattisai *et al*., 2022). Though it appears to have a negative impact on vaccine efficacy and vaccine breakthroughs are expected, there are hopes for T-cell-mediated protection from severe disease in the event that vaccines do not fully fail. The combination of several mutations can increase the binding affinity several folds, for instance, Q498R in combination with N501Y mutation showed a 26-fold increased affinity (Dejnirattisai *et al*., 2022).

There are restrictions on ACE2 folding and binding, according to a recent SARS-CoV-2 RBD mutational screening (Starr *et al*., 2020). Multiple modifications, including those in the ACE2 interface residues that varied between coronaviruses connected to SARS, increased or maintained RBD production and ACE2 binding despite the fact that the majority of these mutations were harmful (Starr *et al*., 2020).

Table 1. List of mutations in Omicron RBD and their impact on the binding free energy ΔΔGBind (kcal/mol). The values were estimated by the BeAtMuSiC server

No. (spike)	No. (RBD)	ΔΔGBind (kcal/mol)	At the RBD/ACE2 interface.
G339D	G6D	-0.07	No
S371L	S38L	-0.08	No
S373P	S40P	0.32	No
S375F	S42F	0.25	No
K417N	K84N	0.27	Yes
N440K	N107K	-0.07	No
G446S	G113S	0.97	Yes
S477N	S144N	0.08	No
T478K	T145K	0.31	No
E484A	E151A	-0.02	Yes
Q493R	Q160R	0.71	Yes
G496S	G163S	0.36	Yes
Q498R	Q165R	0.55	Yes
N501Y	N158Y	-0.08	Yes
Y505H	Y172H	1.43	Yes

Protein-protein docking

Molecular modeling tools are gold standards in microbial evolution and drug discovery against selected molecular targets (Kandeel *et al*., 2021a,b; Mahmoud Kandeel Elsayed, 2021). Figure 3 shows the docking of Omicron RBD with ACE2 receptor. Wt SARS-CoV-2 and its Omicron variant have a 92.27% sequence identity. Nonetheless, mutations in Omicron RBD, as well as the high sequence identity of wt SARS-CoV-2 and its Omicron variant, resulted in a slight increase in RMSD of the Omicron structural model during protein-protein docking, as indicated by the wt SARS-CoV-2 and Omicron RBD-ACE2 complexes RMSD of 0.47 and 0.85 Å, respectively (Fig. 3b).

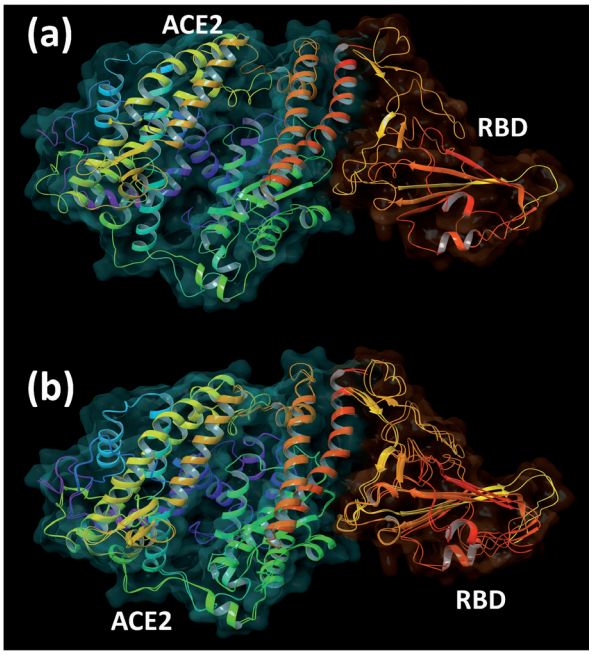

Fig. 3

Protein-protein docking of RBD and ACE2
(a) The produced model for RBD binding with ACE2. **(b)** Alignment of Omicron and wt SARS-CoV-2 RBD-ACE2 structures.

The mutations caused a slight increase in Omicron structure RMSD.

Analysis of mutations impact on the binding force by BeAtMuSiC server

Table 1 summarizes the mutations in Omicron structure and its calculated changes in the binding free energy estimated by the BeAtMuSiC server. The effect of point mutations on binding free energy was almost negative, with five variants related to negative ΔΔGBind, namely G6D, S38L, N107K, E151A, and N158Y, indicating improved binding strength. As a result of the mutations discovered in RBD, ten mutations were projected to decrease binding affinity and five mutations to increase the binding affinity of Omicron RBD and ACE2. While experimental data on Omicron infectivity continue to expand, recombinant Omicron proteins are currently being produced in order to determine their ACE2 binding affinity. A limitation of this technique is that it does not incorporate all probable mutations into a single estimate of affinity alterations. Rather, it examines the impact of specific alterations. As a result, an energy maturation experiment that includes all previously identified RBD mutations could reveal altered binding strength.

In order to examine the binding interactions between the human ACE2 protein and Omicron RBD, atomistic MD simulations have been performed (Lupala *et al.*, 2022). Researchers have found a stronger affinity between the human ACE2 protein and the Omicron RBD strain. By boosting hydrogen bonding contact and expanding hidden solvent accessible surface area, the

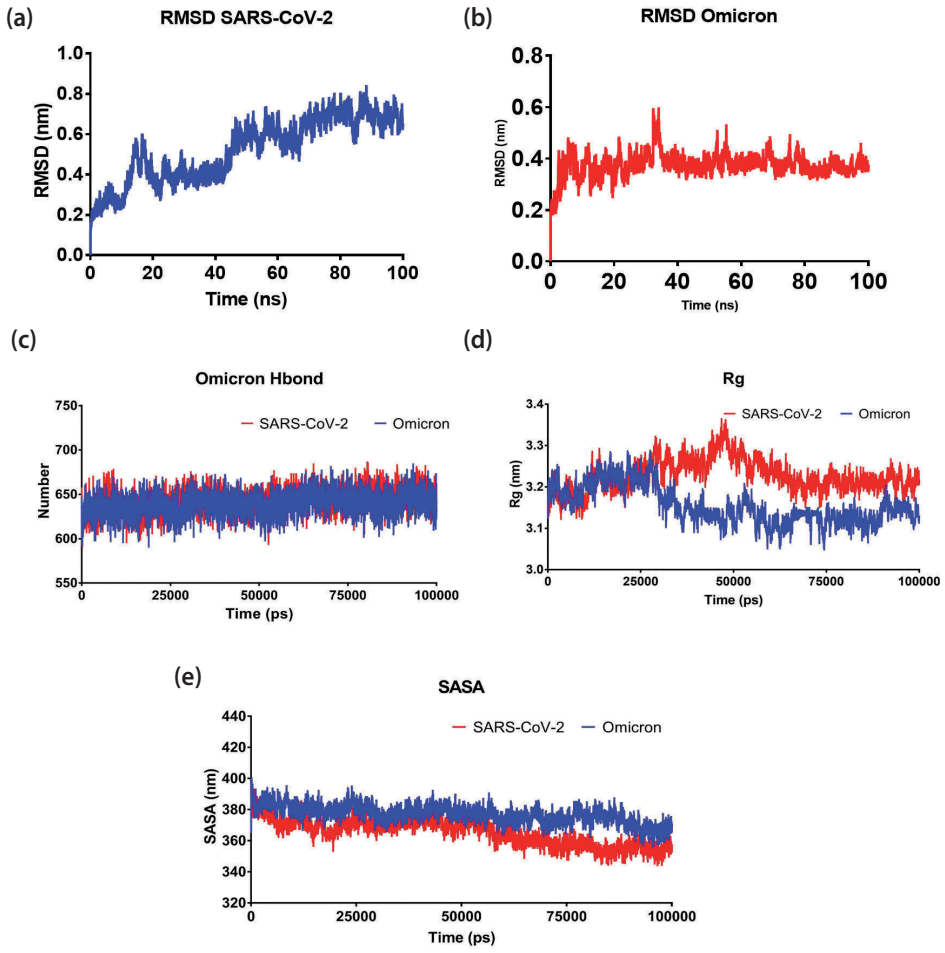

Fig. 4

MD simulations of RBD

(a) The RMSD of wt SARS-CoV-2 RBD-ACE2 complex during 100 ns MD simulation. **(b)** The RMSD of Omicron RBD-ACE2 complex during 100 ns MD simulation. **(c)** The hydrogen bonds of wt SARS-CoV-2 and Omicron RBD-ACE2 complex during 100 ns MD simulation. **(d)** The Rg of wt SARS-CoV-2 and Omicron SARS-CoV-2 and Omicron RBD-ACE2 complex during 100 ns MD simulation. **(e)** The SASA of wt SARS-CoV-2 and Omicron SARS-CoV-2 and Omicron RBD-ACE2 complex during 100 ns MD simulation.

alterations at the ACE2-RBD interface improve tight binding.

Comparison of wt SARS-CoV-2 and Omicron RBD-ACE2 stability and compactness

After 100 ns of MD simulation, it was evident that the Omicron RBD-ACE2 complex had more stable binding than the wt SARS-CoV-2. The RMSD of the alpha carbon atom of the RBD-ACE2 complexes is shown in Fig. 4a,b. The Omicron structure exhibits a smaller RMSD and gained stability faster than the wt SARS-CoV-2 structure, as seen in the image. The average RMSD for Omicron and wt SARS-CoV-2 structures were 0.357 and 0.523 nm, respectively. This displays Omicron's reduced RMSD value and greater stability. During the simulation, both structures formed nearly identical hydrogen bonds (Fig. 4c). The Omicron RBD-ACE2 complex had lower Rg values (Fig. 4d), indicating that both structures are compact and that the Omicron structure has greater structure compactness. During the simulation, the Omicron SASA structure was slightly larger than the wt SARS-CoV-2 structure, as a result of the Omicron mutations (Fig. 4e). Owing to a large number of mutations in Omicron RBD, SASA of wt SARS-CoV-2 structure cannot be compared with the Omicron structure.

The wt SARS-CoV-2 RBD and ACE2 receptors have been studied using computational modeling and dynamic simulations. The Omicron RBD and ACE2-RBD complexes according to the MD simulation were well-defined and stable (Kandeel and El-Deeb, 2022; Wang *et al*., 2020).

Conclusion

Several assumptions were made to predict the Omicron variant's likely emerging pattern, one of which was, that spike mutations boosted the spike's ability to attach to the ACE2 receptor on the host cells. The Omicron variant binding has suggested a stable binding with ACE2 in this work using several methods. Within 15 mutations, only five mutations had negative free energy and support the strong binding, albeit 10 other mutations negatively contributed to the binding. The MD simulation supports the premise that Omicron RBD is more likely to show stable structures than wt SARS-CoV-2 RBD with ACE2. Within these parameters, lower RMSD and higher Rg indicate the proper Omicron structure 3D folding and stability. The higher Omicron structure SASA might also suggest altered interaction with receptor binding and modulation of the virus entry process.

Acknowledgment. This work was supported through the Annual Funding track by the Deanship of Scientific Research, Vice Presidency for Graduate Studies and Scientific Research, King Faisal University, Saudi Arabia [Project No. AN00021].

References

Dehouck Y, Kwasigroch JM, Rooman M, Gilis D (2013): BeAtMuSiC: Prediction of changes in protein-protein binding affinity on mutations. Nucleic Acids Res. 41, W333–9. https://doi.org/10.1093/nar/gkt450

Dejnirattisai W, Huo J, Zhou D, Zahradnik J, Supasa P, Liu C, Duyvesteyn HME, Ginn HM, Mentzer AJ, Tuekprakhon A, Nutalai R, Wan B, Dijokaite A, Khan S, Avinoam O, Bahar M, Skelly D, Adele S, Johnson SA, Amini A, Ritter TG, Mason C, Dold C, Pan D, Assadi S, Bellass A, Omo-Dare N, Koeckerling D, Flaxman A, Jenkin D, Aley PK, Voysey M, Costa Clemens SA, Naveca FG, Nascimento V, Nascimento F, Fernandes da Costa C, Resende PC, Pauvolid-Correa A, Siqueira MM, Baillie V, Serafin N, Kwatra G, Da Silva K, Madhi SA, Nunes MC, Malik T, Openshaw PJM, Baillie JK, Semple MG, Townsend AR, Huang KA, Tan TK, Carroll MW, Klenerman P, Barnes E, Dunachie SJ, Constantinides B, Webster H, Crook D, Pollard AJ, Lambe T, Consortium O, Consortium IC, Paterson NG, Williams MA, Hall DR, Fry EE, Mongkolsapaya J, Ren J, Schreiber G, Stuart DI, Screaton GR (2022): SARS-CoV-2 Omicron-B.1.1.529 leads to widespread escape from neutralizing antibody responses. Cell 185, 467–484 e15. https://doi.org/10.1101/2021.12.03.471045

Gao SJ, Guo H, Luo G (2022): Omicron variant (B.1.1.529) of SARS-CoV-2, a global urgent public health alert! J. Med. Virol. 94, 1255–1256. https://doi.org/10.1002/jmv.27491

Greaney AJ, Starr TN, Gilchuk P, Zost SJ, Binshtein E, Loes AN, Hilton SK, Huddleston J, Eguia R, Crawford KHD, Dingens AS, Nargi RS, Sutton RE, Suryadevara N, Rothlauf PW, Liu Z, Whelan SPJ, Carnahan RH, Crowe JE Jr., Bloom JD (2021): Complete mapping of mutations to the SARS-CoV-2 spike receptor-binding domain that escape antibody recognition. Cell Host Microbe 29, 44–57 e9. https://doi.org/10.1016/j.chom.2020.11.007

He J, Tao H, Yan Y, Huang SY, Xiao, Y (2020): Molecular mechanism of evolution and human infection with SARS-CoV-2. Viruses 12, 428. https://doi.org/10.3390/v12040428

Ho D, Wang P, Liu L, Iketani S, Luo Y, Guo Y, Wang M, Yu J, Zhang B, Kwong P, Graham B, Mascola J, Chang J, Yin M, Sobieszczyk M, Kyratsous C, Shapiro L, Sheng Z, Nair M, Huang Y (2021): Increased resistance of SARS-CoV-2 variants B.1.351 and B.1.1.7 to antibody neutralization. Res. Sq. https://doi.org/10.21203/rs.3.rs-155394/v1

Kandeel M, Albusadah K, Alaydaa SH, Albokhadaim I, Alhojaily S, Marzok M (2021a): Insulin from human, camel and farm animals: comparative bioinformatics and molecular dynamics studies. Pakistan Vet. J. 42, 65–73.

Kandeel M, El-Deeb W (2022): Omicron variant receptor-binding domain phylogenetics and molecular dynamics. Comp. Biol. and Med. 146, 105633. https://doi.org/10.1016/j.compbiomed.2022.105633

Kandeel M, Kitade Y, Almubarak A (2020): Repurposing FDA-approved phytomedicines, natural products, antivirals and cell protectives against SARS-CoV-2 (COVID-19) RNA-dependent RNA polymerase. PeerJ. 8, e10480. https://doi.org/10.7717/peerj.10480

Kandeel M, Yamamoto M, Park BK, Al-Taher A, Watanabe A, Gohda J, Kawaguchi Y, Oh-Hashi K, Kwon HJ, Inoue JI (2021b): Discovery of new potent anti-MERS CoV fusion inhibitors. Front. Pharmacol. 12, 685161. https://doi.org/10.3389/fphar.2021.685161

Kearse M, Moir R, Wilson A, Stones-Havas S, Cheung M, Sturrock S, Buxton S, Cooper A, Markowitz S, Duran C, Thierer T, Ashton B, Meintjes P, Drummond A (2012): Geneious Basic: an integrated and extendable desktop software platform for the organization and analysis of sequence data. Bioinformatics 28, 1647–9. https://doi.org/10.1093/bioinformatics/bts199

Li Q, Wu J, Nie J, Zhang L, Hao H, Liu S, Zhao C, Zhang Q, Liu H, Nie L, Qin H, Wang M, Lu Q, Li X, Sun Q, Liu J, Zhang L, Li X, Huang W, Wang Y (2020): The impact of mutations in SARS-CoV-2 spike on viral infectivity and antigenicity. Cell 182, 1284–1294 e9. https://doi.org/10.1016/j.cell.2020.07.012

Lupala CS, Ye Y, Chen H, Su XD, Liu H (2022): Mutations on RBD of SARS-CoV-2 Omicron variant result in stronger binding to human ACE2 receptor. Biochem. Biophys. Res. Comm. 590, 34–41. https://doi.org/10.1016/j.bbrc.2021.12.079

Mahmoud Kandeel Elsayed AYA-T, Hyung-Joo Kwon, Mohammed Al-Nazawi (2021): MERS-CoV inhibitor peptides. United States Patent Office, Patent No. US10975126B1.

Shu Y, McCauley J (2017): GISAID: Global initiative on sharing all influenza data – from vision to reality. Euro Surveillance 22, 30494. https://doi.org/10.2807/1560-7917.ES.2017.22.13.30494

Starr TN, Greaney AJ, Hilton SK, Ellis D, Crawford KHD, Dingens AS, Navarro MJ, Bowen JE, Tortorici MA, Walls AC, King NP, Veesler D, Bloom JD (2020): Deep mutational scanning of SARS-CoV-2 receptor binding domain reveals constraints on folding and ACE2 binding. Cell 182, 1295–1310 e20. https://doi.org/10.1016/j.cell.2020.08.012

Wang L, Cheng G (2022): Sequence analysis of the emerging SARS-CoV-2 variant Omicron in South Africa. J. Med. Virol. 94, 1728–1733. https://doi.org/10.1002/jmv.27516

Wang Y, Liu M, Gao J (2020): Enhanced receptor binding of SARS-CoV-2 through networks of hydrogen-bonding and hydrophobic interactions. PNAS 117, 13967–13974. https://doi.org/10.1073/pnas.2008209117

Waterhouse A, Bertoni M, Bienert S, Studer G, Tauriello G, Gumienny R, Heer FT, de Beer TAP, Rempfer C, Bordoli L, Lepore R, Schwede T (2018): SWISS-MODEL: homology modelling of protein structures and complexes. Nuc. Acids Res. 46, W296-W303. https://doi.org/10.1093/nar/gky427

Yan Y, Tao H, He J, Huang SY (2020): The HDOCK server for integrated protein-protein docking. Nature Prot. 15, 1829–1852. https://doi.org/10.1038/s41596-020-0312-x

Zahradnik J, Marciano S, Shemesh M, Zoler E, Harari D, Chiaravalli J, Meyer B, Rudich Y, Li C, Marton I, Dym O, Elad N, Lewis MG, Andersen H, Gagne M, Seder RA, Douek DC, Schreiber, G (2021): SARS-CoV-2 variant prediction and antiviral drug design are enabled by RBD in vitro evolution. Nat. Microbiol. 6, 1188–1198. https://doi.org/10.1038/s41564-021-00954-4

Zhang L, Li Q, Liang Z, Li T, Liu S, Cui Q, Nie J, Wu Q, Qu X, Huang W, Wang Y (2022): The significant immune escape of pseudotyped SARS-CoV-2 variant Omicron. Emerg. Microbes Inf. 11, 1–5. https://doi.org/10.1080/22221751.2021.2017757